Journal of Catalysis **199,** 318–327 (2001)
doi:10.1006/jcat.2001.3170, available online at http://www.idealibrary.com on IDEAL®

# An XAFS Study of the Different Influence of Chelating Ligands on the HDN and HDS of $\gamma$-$Al_2O_3$-Supported NiMo Catalysts

Riccardo Cattaneo, Fabio Rota, and Roel Prins[1]

*Laboratory for Technical Chemistry, Federal Institute of Technology (ETH), 8092 Zurich, Switzerland*

Received October 12, 2000; revised January 8, 2001; accepted January 9, 2001; published online March 21, 2001

**$\gamma$-$Al_2O_3$-supported NiMo catalysts prepared in the presence of the chelating ligands nitrilotriacetic acid (NTA) and ethylenediamine tetraacetic acid (EDTA) were tested in the hydrodenitrogenation (HDN) of o-toluidine and in the hydrodesulfurization (HDS) of thiophene. For the molar ratio NTA : Ni = 1 a maximum was observed in the HDN activity, but a minimum activity was observed in the HDS and in the hydrogenation of cyclohexene. The highest HDS activities were obtained for the calcined catalyst prepared in the absence of ligands and for the catalyst prepared with EDTA. The Mo *K*-edge Quick EXAFS and normal EXAFS data demonstrated that in the catalysts with the highest HDN activity $MoS_2$ is formed at the lowest temperature and the $MoS_2$ crystallites have the highest structural order. This suggests that o-toluidine can adsorb better on $MoS_2$ crystallites with more regular edges. The increase in HDS activity was ascribed to a change in the mechanism of sulfidation of Ni, induced by the chelating ligands, and to a subsequently higher dispersion of Ni. Mo-oxysulfides could not be distinguished by Quick EXAFS during sulfidation of Mo. The Quick EXAFS data indicate that a $MoS_3$-like phase precedes $MoS_2$ during the sulfidation process. The chelating ligands *screen* the Ni cations and prevent their interactions with the environment. In the absence of chelating ligands, Ni interacts with the support and changes its surface properties. In this way the Mo–support interactions and the sulfidation of Mo are affected. The influence of the chelating ligands on the sulfidation of Mo suggests that the sulfidation process of Mo is closely dependent on the sulfidation of Ni.** © 2001 Academic Press

*Key Words:* **hydrodesulfurization; hydrodenitrogenation; alumina; chelating ligands; EXAFS; Quick EXAFS.**

## INTRODUCTION

In previous studies (1–9) the effects of the chelating ligands on $SiO_2$-supported catalysts were investigated. The addition of chelating ligands during the preparation of hydrotreating catalysts leads to catalysts with higher˜activity (1, 2). Alumina is still the support of choice in industrial applications, however, because of the stronger interactions between the metal sulfides and the support,which induce a more stable catalyst at elevated temperatures (1, 2). Therefore, we investigated the catalytic performance of $NiMo/Al_2O_3$ catalysts, prepared in the presence of chelating ligands, during hydrodenitrogenation (HDN) and hydrodesulfurization (HDS). Quick EXAFS (QEXAFS) spectra were measured during the sulfidation of catalysts to study the sulfidation process of Mo and Ni in the presence and absence of the chelating ligand. In addition to QEXAFS measurements of the sulfidation, normal EXAFS spectra of the sulfided catalysts were measured as well to determine the structural features that influence the activity of the studied materials.

In this study, we chose the HDN of toluidine, the HDS of thiophene, and the hydrogenation of cyclohexene to test the hydrotreating properties of the catalysts. HDN is an important step in hydrotreating. Several authors studied the activity and structure of the catalysts (10) as well as the mechanisms and the kinetics of the HDN reaction (11, 12). o-Toluidine was chosen as a model compound, because its network (Fig. 1) contains the most important reactions that take place in HDN: o-Toluidine (TOL) can be hydrogenated to 2-methylcyclohexylamine (2-MCHA) or it can react to toluene (T). Under the conditions of our study, T could not react further, as was shown by the fact that its selectivity did not depend on conversion (13, 14). 2-MCHA reacts via elimination to methylcyclohexene (MCHE) that can react further via hydrogenation of the double bond to the final product methylcyclohexane (MCH). MCHA can also react directly to MCH via nucleophilic substitution of the amine group by a sulfhydril group, followed by hydrogenolysis of 2-methylcyclohexanethiol (MCHT) (15).

Hydrodesulfurization has been the subject of numerous reviews (16–18). Thiophene is often used to test the HDS catalytic activity (5, 19). Its network is relatively simple at elevated $H_2$ pressures, the major reaction path going via hydrogenation of thiophene to tetrahydrothiophene (20). This intermediate can react to butadiene through two $\beta$-H eliminations. At high $H_2$ pressure, butadiene quickly reacts further to 1-butene, 2-butene (*cis* and *trans*), and eventually to butane. The HDS mechanism of thiophene at atmospheric pressure is still under debate. Several authors have

[1] To whom correspondence should be addressed. E-mail: prins@tech.chem.ethz.ch.



0021-9517/01 $35.00

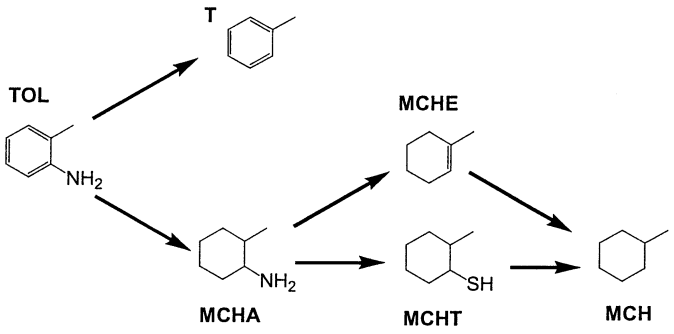


**FIG. 1.** Reaction network of the HDN of o-toluidine.

proposed that the hydrogenolysis path through butadiene is the major route (21, 22). A direct pathway for the hydrodesulfurization of thiophene to butene has been suggested on the basis of the absence of tetrahydrothiophene (23). It has been revealed that hydrogenated S-intermediates are present, suggesting that parallel paths exist (24) or that prehydrogenation may be necessary before C–S bond cleavage occurs (25). Organometallic studies have suggested that a pathway via 2,5-dihydrothiophene might also be feasible (26, 27).

## EXPERIMENTAL

### *Catalyst Preparation*

The catalysts used in this work contained about 7 wt% Mo and 2.5 wt% Ni and were prepared by pore volume coimpregnation of $\gamma$-$Al_2O_3$ (CONDEA, pore volume: 0.5 $cm^3/g$, specific area: 100 $m^2/g$) with an aqueous solution (pH 9.5) of $(NH_4)_6Mo_7O_{24} \cdot 4H_2O$ (Aldrich) and $Ni(NO_3)_2 \cdot 6H_2O$ (Aldrich) with 25% ammonia in the presence or absence of the chelating ligands nitrilotriacetic acid (NTA) (Fluka) and ethylenediamine tetraacetic acid (EDTA) (Fluka). Ammonia must be used in the preparation of catalysts containing the chelates (1, 2). It was therefore also used in the absence of chelates in order to obtain comparable materials. The support was dried at 120°C for 12 h prior to impregnation. The impregnated powder was dried in air at ambient temperature for 4 h and dried in an oven at 120°C for 15 h. Calcination was carried out only for the catalyst prepared without ligands at 500°C for 4 h. For all other catalysts, calcination was omitted to avoid the decomposition of the metal–ligand complexes in the catalyst precursors. The investigated catalysts are listed in Table 1.

### *HDN Activity Tests*

The oxidic precursor (70 mg) was diluted with 8 g SiC to achieve plug-flow conditions in the continuous-flow, fixed-bed reactor. The catalyst was sulfided *in situ* with a mixture of 10% $H_2S$ in $H_2$ at 400°C and 1.0 MPa for 2 h. After sulfidation, the pressure was increased to 5.0 MPa and the liquid reactant was fed to the reactor by means of a high-pressure syringe pump (ISCO 500D). All reactions were performed at 370°C. Dimethyldisulfide (DMDS) was added to the liquid feed to generate $H_2S$ in the reaction stream. o-Toluidine was used as a model compound to study the HDN reaction, and cyclohexene was added to the feed to study the hydrogenation reaction. The composition of the gas phase reactant for the catalytic tests was 7 kPa of o-toluidine, 4 kPa of cyclohexene, 4800 kPa of $H_2$, 134 kPa of octane, 20 kPa heptane (reference), and 17.5 kPa of $H_2S$.

The reaction products were analyzed by online gas chromatography with a Varian 3800 GC instrument equipped with a 30-m DB-5 fused silica capillary column (J & W Scientific, 0.32 mm i.d., 0.25 $\mu$m film thickness), a flame ionization detector (FID), and a pulsed flame photometric detector (PFPD). Space time was defined as $\tau = w_c/n_{feed}$, where $w_c$ denotes the catalyst weight and $n_{feed}$ the total molar flow fed to the reactor. The space time ($\tau$) was changed by varying the liquid and gaseous reactant flow rates, while their relative ratios were kept constant.

### *HDS Activity Tests*

The oxidic precursor (100 mg) was mixed with 1 g of SiC and sulfided with a mixture of 10% $H_2S$ in $H_2$ (Messer Griesheim), starting at room temperature and heating to 400°C at a rate of 6°C/min. The sulfidation was finished with 2 h sulfidation at 400°C. The activity of all catalysts was tested in the hydrodesulfurization of thiophene at 370°C. The feed (3% thiophene in $H_2$) was obtained by bubbling $H_2$ through a series of four thiophene saturators that were cooled to 2°C. The product stream was analyzed online with an HP5890 gas chromatograph. The sulfidation of the oxidic precursors and the thiophene HDS reactions occurred at atmospheric pressure.

### *XAFS Measurements*

The Quick EXAFS measurements were carried out at the X1 (RÖMO II) beam line at HASYLAB (Hamburg, Germany) (7, 28). Si (311) and Si (111) crystals were used in the monochromator for the Mo and Ni *K*-edges, respectively.

**TABLE 1**

**List of Catalysts Used in This Work**

| Catalyst | Loading (wt%) | | Ligand : Ni (molar ratio) |
|---|---|---|---|
| | Mo | Ni | |
| NiMo calcined | 6.8 | 2.6 | 0.0 |
| NiMo not calcined | 6.9 | 2.5 | 0.0 |
| NiMoNTA 0.5 | 6.0 | 2.2 | 0.5 |
| NiMoNTA 1.0 | 5.8 | 2.2 | 1.0 |
| NiMoNTA 1.5 | 6.0 | 2.2 | 1.5 |
| NiMoEDTA | 6.0 | 2.2 | 1.0 |

The accumulation time was about 0.2 s/step at the Mo *K*-edge and about 0.4 s/step at the Ni *K*-edge. The *k*-ranges used for the analysis of the data were 3–17 $Å^{-1}$ for the Mo and 3–12 $Å^{-1}$ for the Ni *K*-edge. The normal EXAFS spectra were collected at the Swiss Norwegian Beam Line at the European Synchrotron Radiation Facility (ESRF) in Grenoble, France (5). The *k*-range used for the analysis of the data was 3–19.5 $Å^{-1}$ for the Mo *K*-edge and 3–16 $Å^{-1}$ for the Ni *K*-edge.

For both kinds of measurements, the catalyst samples were pressed into self-supporting wafers and mounted in an *in situ* EXAFS cell (29). The thickness of the samples was chosen to adjust the edge jump to 1 for the Mo *K*-edge and the total absorption to $\mu x = 4$ for the Ni *K*-edge (lower Ni concentration). For the QEXAFS measurements, two spectra of the fresh samples in an atmosphere of He were collected. The samples were then sulfided *in situ* during data collection. A stream of 10% $H_2S/H_2$ flowed through the cell while it was heated to 400°C at a rate of 3°C/min. For classical EXAFS measurements, the samples were cooled to room temperature after sulfidation at 400°C for 0.5 h. Different conditions were used for the sulfiding processes preceding the catalytic tests (6°C/min, 2 h) and the EXAFS measurements (3°C/min, 0.5 h). These differences were chosen in order to improve the quality of the QEXAFS data and to reduce the collection time at 400°C. Previous experiments showed that these differences do not affect the sulfidation mechanism of Ni and of Mo (7). In the same work, an isothermal experiment was carried out, which showed that no significant difference could be noticed in the parameters obtained from the EXAFS spectra if the catalyst was kept at a constant temperature for 0.5 or for 2 h.

Once at room temperature, the $H_2S$ still present in the cell was replaced by He by flushing for 10 min. The cell was then cooled to liquid nitrogen temperature prior to the EXAFS measurement.

The program XDAP (version 2.2.2) (30) was used to analyze and fit the data as described in (5, 7). Apart from references for Mo–S and Mo–Mo, which were obtained from the experimental EXAFS spectrum of $MoS_2$, reference spectra were calculated using the Feff7 code (31, 32).

## RESULTS

### *Catalytic Performance*

*HDN and HYDR activity.* The HDN of o-toluidine (TOL), as a function of space time, shows that toluene (T) and 2-methylcyclohexylamine (MCHA) are primary products (cf. Fig. 1). The selectivity of toluene (T) as a function of conversion is constant for all catalysts tested and amounted to about 5 to 10% of the total conversion. It proves that T is produced in parallel to the other products (13). The produced MCHA reacts so quickly that it is only observed in trace amounts when the HDN of TOL is carried out alone (15).

**TABLE 2**

**Conversion (in %) in the HDN of Toluidine, the Hydrogenation of Cyclohexene, and the HDS of Thiophene**

| Catalyst | HDN | HYDR | HDS |
|---|---|---|---|
| NiMo calcined | 54 | 88 | 32 |
| NiMo not calcined | 52 | 70 | 22 |
| NiMoNTA 0.5 | 60 | 65 | 21 |
| NiMoNTA 1.0 | 83 | 70 | 18 |
| NiMoNTA 1.5 | 66 | 94 | 25 |
| NiMoEDTA | 63 | 92 | 32 |

Table 2 presents the results of the HDN of TOL with the different catalysts investigated in this work. No significant difference in the HDN activity was observed between the calcined and the dried catalysts prepared in the absence of chelating ligands. This comparison was made because calcined catalysts are usually employed in industrial applications and catalysts prepared with chelating ligands cannot be calcined. The addition of NTA induced an increase in catalytic activity until a maximum was obtained for the catalyst with the molar ratio NTA : Ni = 1, which is about 55% more active than the catalyst prepared without ligands. The addition of EDTA had the same effect as NTA at an NTA : Ni = 1.5 ratio.

The behavior of the conversion of CHE for the different catalysts is very different to that of the TOL reaction. Whereas the catalysts prepared in the presence of chelating ligands are more active in HDN than those prepared without ligands, in the hydrogenation of cyclohexene the activities of the catalysts prepared with NTA at NTA : Ni ratios of 0.5 and 1.0 were lower than that of the calcined catalyst. Increasing the NTA loading led to a continuous increase in the conversion of CHE, so that the activity of the NiMoNTA 1.5 catalyst was somewhat higher than that of the calcined catalyst. The catalyst prepared with EDTA had the same activity as the NTA : Ni = 1.5 catalyst.

*HDS activity.* The HDS activities follow more or less the same pattern as the hydrogenation activities (cf. Table 2). The activity of the calcined catalyst is significantly higher than that of the dried catalyst prepared in the absence of ligands. The effect of the addition of NTA depends on the amount of the chelating ligand used. For the NiMoNTA 0.5 and NiMoNTA 1.0 catalysts, a decrease in activity is observed relative to the uncalcined NiMo catalyst, whereas the activity of the NiMoNTA 1.5 catalyst was slightly larger than that of the uncalcined NiMo catalyst. The catalyst prepared with EDTA had an even higher activity than the NiMoNTA 1.5 catalyst, comparable to that of the calcined NiMo catalyst.

Although NTA did not improve the HDS activity, it is interesting to compare the HDS results with the results obtained for the HDN of TOL and the hydrogenation of CHE. The catalyst showing the lowest HDS activity is the most active in the HDN reaction. Similarly, the catalysts showing the highest HDS activity are not particularly active in the HDN of TOL. A comparison of the HDS and the hydrogenation reactions shows that the catalysts behave more or less the same for both reactions. The catalysts containing NTA with the molar ratio NTA : Ni = 0.5 and 1 are the least active catalysts while the calcined catalysts, NiMoNTA 1.5 and NiMoEDTA, are the most active.

The three reactions investigated in this work follow different pathways. The data presented in Table 2 show that a change in the structure of the catalyst accelerates some reactions and decelerates others. It is not possible to say that an increase of the HDS activity implies a decrease of the HDN performance or vice versa also because the first reaction was carried out at atmospheric pressure while the second at higher pressure. It might, however, be possible to understand which structural characteristics are more important for the different reaction patterns. The QEXAFS and classical EXAFS data may show which of the features in the sulfidation behavior and in the structure of the final catalysts are responsible for the observed differences in catalytic performance for the studied reactions.

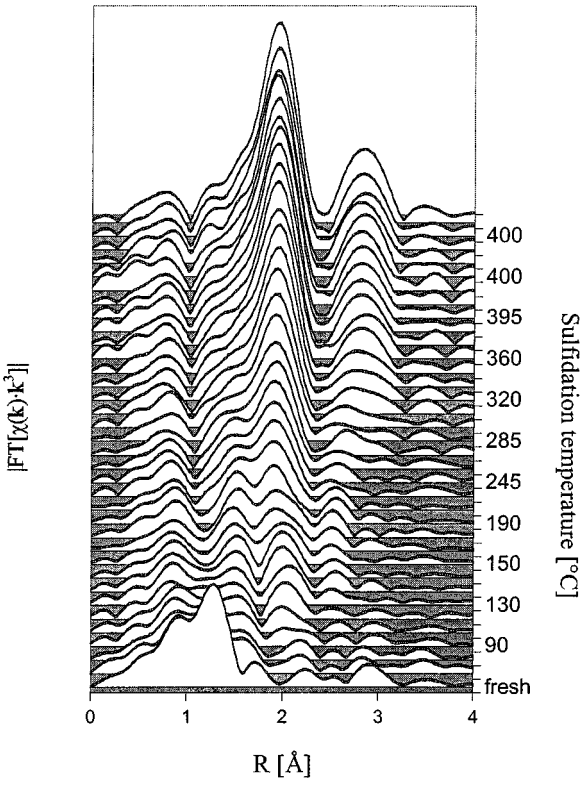


**FIG. 2.** Mo *K*-edge QEXAFS spectra collected during the sulfidation of the calcined NiMo catalyst.

*Catalyst Characterization*

*MoK-edge Quick EXAFS.* In Fig. 2, the QEXAFS spectra measured during the sulfidation of the calcined $NiMo/Al_2O_3$ catalyst are plotted against the sulfidation temperature. In the spectrum of the fresh catalyst, Mo–O contributions between 0.8 and 2 Å (phase uncorrected) and a Mo–Mo shell at 3 Å (not phase corrected) can be recognized. The latter shell suggests the presence of polymolybdates in the catalyst precursor. The nature of the signal at 2.2 Å (not phase corrected) is not clear.

The effect of sulfidation becomes apparent in the spectrum measured at 50°C, in which the amplitude of the Mo–O signal has decreased compared with the spectrum of the fresh catalyst. In the spectrum measured around 105°C, a Mo–S signal appears at a distance of 2 Å (phase uncorrected) from the absorber atom. Another signal increases its intensity at 2.5 Å (phase uncorrected) at around the same temperature. The same signal was observed in $SiO_2$-supported NiMo catalysts and was attributed to a Mo–Mo shell of the $MoS_3$-like product of the sulfidation of molybdenum (7). The Mo–S and the Mo–Mo signals increase with increasing sulfidation temperature, but at around 255°C the Mo–Mo shell starts to shift toward larger distance. At this temperature, $MoS_2$ starts to form and two Mo–Mo signals overlap, one belonging to the $MoS_3$-like material and the other to the Mo-Mo shell of $MoS_2$ at 3.16 Å. After 0.5 h sulfiding at 400°C the Mo–O signal is still clearly present.

The sulfidation of Mo in the $NiMoNTA/Al_2O_3$ catalyst with the molar ratio NTA : Ni = 1 is presented in Fig. 3. The QEXAFS spectra show that the sulfidation of Mo in this catalyst is very similar to that in the calcined catalyst. Nevertheless, for the spectra collected between 205 and 260°C, a decrease is observed in the Mo–S signal at 2 Å (not phase corrected). Analyses of the QEXAFS spectra with a Mo–S and a Mo–Mo shell showed that, in this temperature range, the Mo–S coordination number first decreases and then increases again. A similar behavior was observed for all dried catalysts. Figure 4 shows the Mo–S coordination numbers obtained by fitting the QEXAFS spectra as a function of the sulfidation temperature for the various catalysts. A maximum is present for every catalyst, after which a decrease is observed, corresponding to the decrease in the amplitude of the Mo–S signal in the QEXAFS spectra. The maximum is reached at different temperatures for the various catalysts, and at the lowest temperature (215°C) for the NiMoNTA 1.0 catalyst. The other maxima are observed at 240°C for the NiMoNTA 1.5 catalyst, at 255°C for the catalyst prepared without ligands, and at 250 to 260°C for the catalyst prepared with EDTA.

The Mo–S and Mo–Mo distances as observed in the QEXAFS spectra of various catalysts are plotted in Fig. 5 as a function of the sulfidation temperature. This figure shows that, in the same temperature range where the maxima for

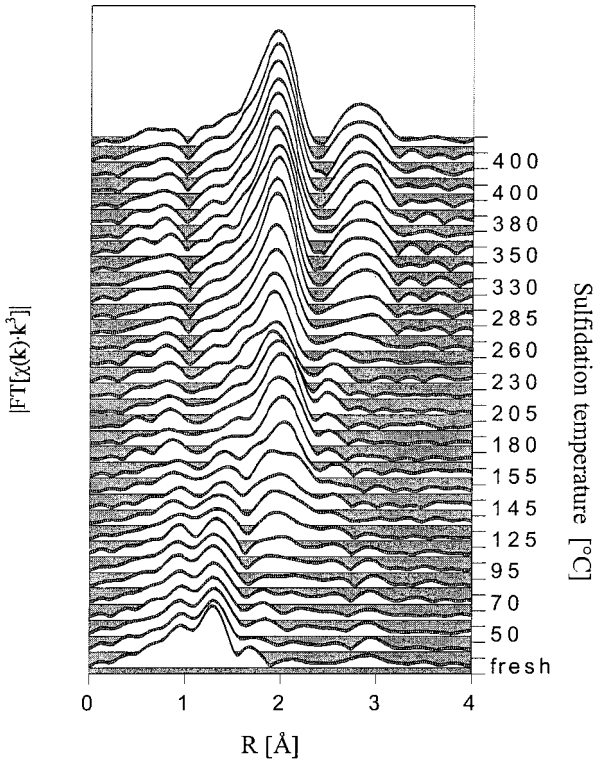


**FIG. 3.** Mo *K*-edge QEXAFS spectra collected during the sulfidation of the NiMoNTA/$Al_2O_3$ catalyst with the molar ratio NTA : Ni = 1.

the Mo–S coordination number were observed, a shift in the Mo–S shell (from 2.49 to 2.42 Å) and in the Mo–Mo shell (from 2.79 to 3.19 Å) is detected. The shift in the Mo–S shell is minor but significant, whereas the change in the Mo–Mo distance is marked. Because of experimental

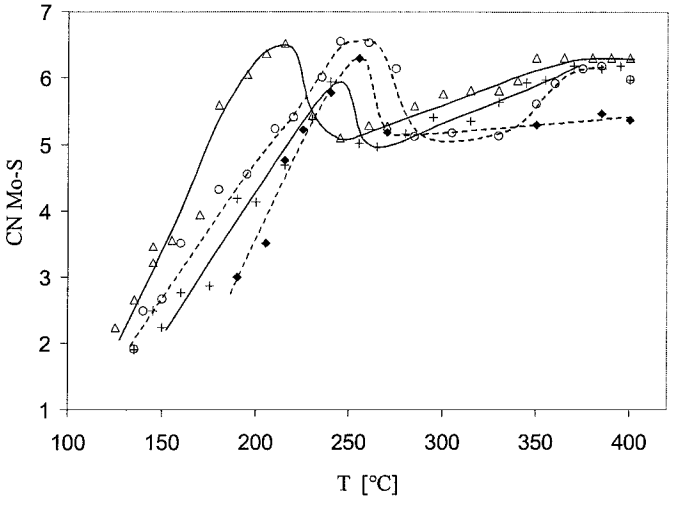


**FIG. 4.** Mo–S coordination number obtained from the fit of the QEXAFS spectra as a function of the sulfidation temperature for the alumina-supported catalysts: (◆) NiMo not calcined, (△) NiMoNTA 1.0, (+) NiMoNTA 1.5, (○) NiMoEDTA.

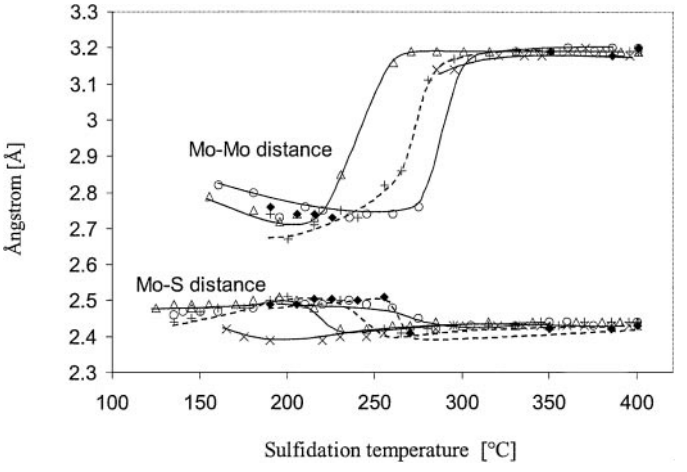


**FIG. 5.** Mo-Mo and Mo–S distances obtained from the QEXAFS spectra as a function of the sulfidation temperature: (◆) NiMo not calcined, (△) NiMoNTA 1.0, (+) NiMoNTA 1.5, (○) NiMoEDTA, (×) NiMo calcined.

problems, the spectra of the sulfidation of the catalyst containing no ligands were not measured in the region between 270 and 350°C. Nevertheless, it is clear that this catalyst follows the same trend. In the NiMoNTA 1.0 catalyst, the shift in the distances takes place at the lowest temperature, whereas the catalyst prepared with EDTA goes through this step at the highest temperature. The final distances of 2.42 Å for the Mo–S shell and 3.19 Å for the Mo–Mo shell are very close to the corresponding distances of 2.42 and 3.16 Å in $MoS_2$. We found, therefore, a precise method for detecting the moment that $MoS_2$ is first present in our catalyst during the sulfidation process. The next step consists of determining the consequences of this shift in the temperature of formation of $MoS_2$ for the structure of the final catalysts. For that reason, we measured classical EXAFS spectra which will enable us to investigate the structural features of the sulfided catalysts.

As far as the beginning of the sulfidation is concerned, no clear difference was found between the various catalysts. During the sulfidation of Mo in silica-supported NiMo catalysts, two intermediates were detected, an oxysulfide and a $MoS_3$-like material (signal at 2.5 Å) (7). On alumina, the $MoS_3$-like material starts to form at lower temperatures than on silica. It is possible that molybdenum oxysulfide and the $MoS_3$-like compound are present in the same temperature range. The fact that Mo–O, Mo–S, and Mo–Mo shells are observed in the same spectra does not, however, allow one to distinguish molybdenum oxysulfides from the features of the collected QEXAFS spectra.

*Mo K-edge EXAFS.* Classical EXAFS spectra were collected for three catalysts after 0.5 h sulfidation at 400°C. The quality of the data is seen in Fig. 6, where the $k^3$-weighted $\chi(k)$ data of the dried catalyst that does not contain a ligand are plotted. Note that a very good signal-to-noise ratio was

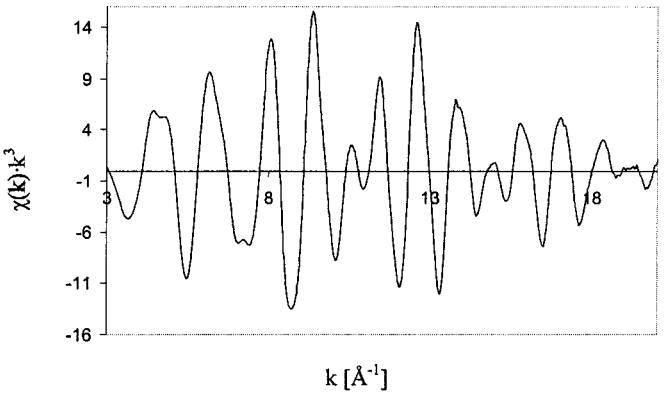


**FIG. 6.** Mo *K*-edge $k^3$-weighted EXAFS function of the dried NiMo catalyst containing no ligands sulfided at 400°C.

obtained up to 20 $Å^{-1}$. The Fourier-transformed data are presented in Fig. 7, in which a difference in the amplitude of the Mo–Mo shell at 2.9 Å (not phase corrected) is clearly observed between the spectra of the uncalcined $NiMo/Al_2O_3$ and those of the NiMoNTA $1.0/Al_2O_3$ and the NiMoNTA $1.5/Al_2O_3$ catalysts. The results of the fits presented in Table 3 reveal that the differences shown in Fig. 7 are primarily due to dissimilar Debye–Waller factors for the Mo–Mo shells. In the catalyst prepared without ligands, the Debye–Waller factor has the highest value, indicating a higher static disorder and a lower crystallinity of the $MoS_2$ particles. The presence of NTA improves the order of the $MoS_2$ slabs. For the NiMoNTA 1.0 catalyst, the Debye–Waller factor of the Mo–Mo shell has the lowest value. There is a clear correlation between the value of the Debye–Waller factor and the sequence of the temperature of formation of $MoS_2$ (see Fig. 4). The lower the formation temperature of $MoS_2$, the lower is the value of the Debye–Waller factor, which indicates a higher static order in the final $MoS_2$ particles. The same trend was observed for $SiO_2$-supported catalysts, but the effect on the Debye–Waller factor was not as marked as here (5, 7). In the present case, the Debye–Waller factor for the Mo–Mo shell of the catalyst prepared in the absence of ligands is twice as large as for the catalyst NiMoNTA 1.0 (Table 3).

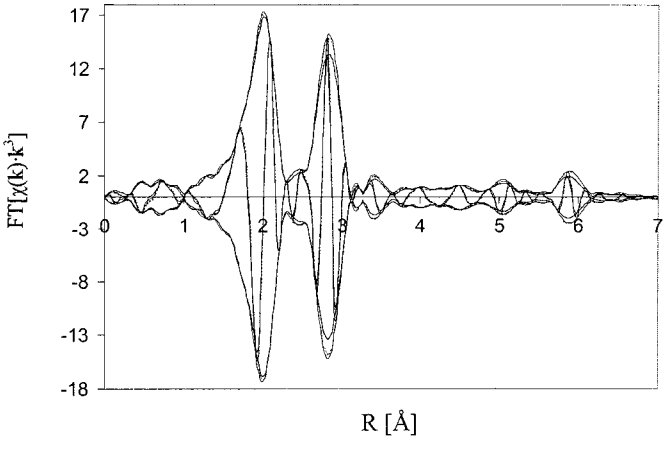


**FIG. 7.** Mo *K*-edge Fourier transformed EXAFS spectra of the sulfided catalysts prepared in the presence and absence of NTA: (inner spectrum) NiMo not calcined, (outer spectrum) NiMoNTA 1.0, (middle spectrum) NiMoNTA 1.5.

**TABLE 3**

**Parameters Obtained from the Fit of the Spectra of the Sulfided $NiMo/Al_2O_3$ Catalysts**

| Catalyst | Shell | CN | $R$ [Å] | $\Delta\sigma^2$ [$10^{-4}$ Å$^2$] | $\Delta E^\circ$ [eV] | Goodness of fit |
|---|---|---|---|---|---|---|
| NiMo not calcined | Mo–S | 5.8 | 2.42 | 5.0 | 3.1 | 0.79 |
| | Mo–Mo | 3.6 | 3.16 | 8.2 | 3.7 | |
| NiMoNTA 1.0 | Mo–S | 6.0 | 2.42 | 5.0 | 3.8 | 0.79 |
| | Mo–Mo | 3.6 | 3.16 | 4.1 | 4.7 | |
| NiMoNTA 1.5 | Mo–S | 5.9 | 2.42 | 4.6 | 4.1 | 0.60 |
| | Mo–Mo | 3.7 | 3.16 | 5.4 | 4.8 | |

As far as the Mo–S shell is concerned, it is noteworthy that the Mo–S coordination number of the catalyst made with NTA with the molar ratio NTA:Ni = 1 amounts to 6.0, whereas for the other catalysts, values slightly below 6 are obtained. This indicates that all the edges of the $MoS_2$ crystallites are saturated with S.

*Ni K-edge QEXAFS.* The sulfidation of Ni in the catalysts was also investigated by means of QEXAFS. Figure 8 shows the sulfidation of Ni in the NiMoNTA 1.0 catalyst as followed by QEXAFS. The spectrum of the catalyst precursor (*fresh*) shows two main signals. The first signal at 1.6 Å (phase not corrected) is produced by the Ni–O shells, whereas the second signal at 2.2 Å (phase uncorrected) is due to the presence of the carbon atoms belonging to the NTA ligands around Ni (5). Careful observation of the first signal enables us to detect when the oxygen atoms around Ni are replaced by sulfur, because the Ni–S distance is about 0.2 to 0.3 Å larger than the Ni–O distance. Moreover, it can be noticed that in the same temperature region in which the shift of the first shell is observed, the Ni–C shell gradually disappears.

A more precise picture of the sulfidation of Ni in the different catalysts is achieved by monitoring the XANES spectra. As can be seen in Fig. 9, the shape of the spectra changes during the sulfidation process. By means of a linear fitting it is possible to estimate the fraction of sulfided Ni in the catalyst (6). The spectra are considered to be a linear combination of the spectrum of the fresh catalyst and the spectrum collected after sulfidation at 400°C. The spectrum of the dried catalyst prepared without ligands after sulfidation was used as a reference for the sulfided state of the calcined catalyst. The results of this procedure are plotted in Fig. 10. The presence of NTA shifts the sulfidation of Ni to lower temperatures relative to the dried catalyst.

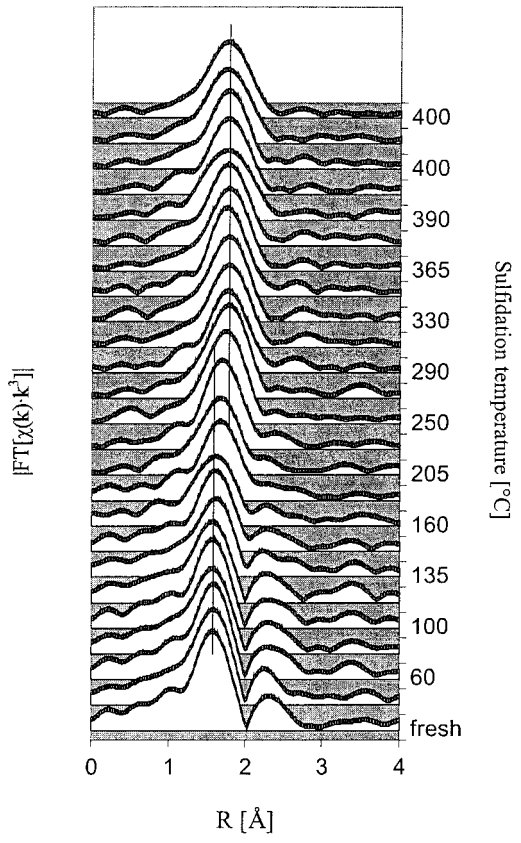


**FIG. 8.** Ni *K*-edge QEXAFS spectra collected during the sulfidation of the NiMoNTA/$Al_2O_3$ catalyst with the molar ratio NTA : Ni = 1.

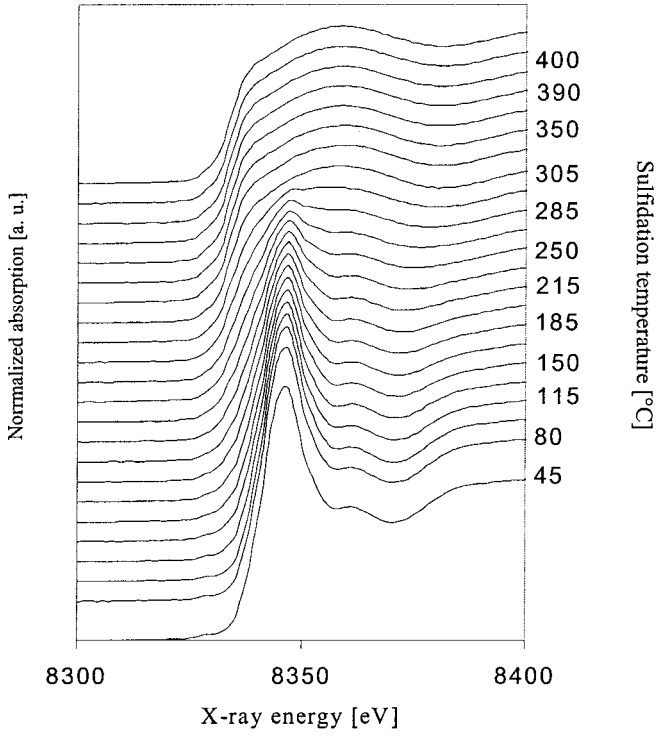


**FIG. 9.** Ni *K*-edge XANES spectra collected during the sulfidation of the dried NiMo catalyst containing no ligands.

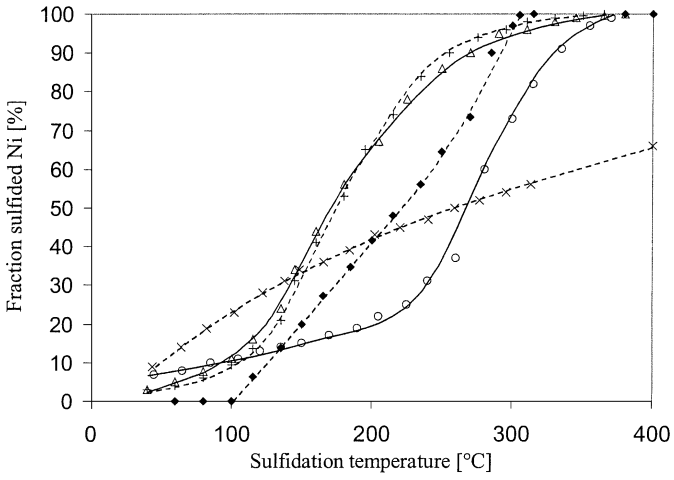


**FIG. 10.** Degree of sulfidation of Ni on the alumina-supported catalysts as obtained from the XANES spectra: (◆) NiMo not calcined, (△) NiMoNTA 1.0, (+) NiMoNTA 1.5, (○) NiMoEDTA, (×) NiMo calcined.

No difference is observed between the two NTA-containing catalysts. On the contrary, EDTA delays the sulfidation of Ni. The behavior of the calcined catalyst is different. In this catalyst, the fraction of sulfided Ni after sulfidation at 400°C for 0.5 h is only about 70%, even though the initial sulfidation rate is fast. This is due to the fact that, during calcination, some of the Ni was incorporated into the support. This fraction of nickel was not sulfided. The EXAFS signal is, therefore, an average of the sulfided Ni present on the surface of the support and of the unsulfided Ni in $\gamma$-$Al_2O_3$.

## DISCUSSION

We will first concentrate on the mechanism of sulfidation of Mo and how it is affected by the ligands. Some considerations on the sulfidation of Ni will then follow. In both cases we will explain how the structural features influence the catalytic performance. In the last section we explain how the chelating ligands affect the structural features of Ni and Mo during the preparation of the catalysts.

### *Molybdenum*

The use of QEXAFS enabled us to distinguish three regions in the sulfidation mechanism of Mo: the oxidic state, an intermediate $MoS_3$-like material, and the final $MoS_2$. This sequence differs from the sequence observed for $SiO_2$-supported catalysts (7). Two intermediate regions were detected on silica, a Mo-oxysulfide and the $MoS_3$-like product. On alumina, the oxysulfide intermediate cannot be clearly distinguished. Because of the high pH of the impregnation solution (9.5), Mo is present on the $Al_2O_3$-supported catalyst precursors mainly as $MoO_4^{2-}$ units, although a fraction is present as polyanions, as the signal at 3 Å suggests. In

contrast , polymolybdates are the main species on $SiO_2$ (5). The smaller molybdate molecules are easier to sulfide, because no Mo–O–Mo bridging bonds have to be cleaved. Therefore, the transformation of the oxidic phase to the $MoS_3$-like material takes place at lower temperatures, and the presence of molybdenum oxysulfides is *hidden* in the QEXAFS spectra by the fast formation of the $MoS_3$-like product.

Furthermore, the behavior of the Mo–S and Mo–Mo shells proves the transformation of the intermediate product to $MoS_2$. The coordination numbers and distances obtained by fitting the QEXAFS data (Figs. 4 and 5) suggest that the intermediate product preceding $MoS_2$ resembles $Mo_2S_{12}^{2-}$ anions (Mo–S coordination number 8, Mo–S distance 2.40–2.49 Å, Mo–Mo distance 2.81 Å (33)) and $Mo_3S_{13}^{2-}$ anions (Mo–S coordination number 7, Mo–S distance 2.35–2.49 Å, Mo–Mo distance 2.71 Å (34)). The possibility of fitting the QEXAFS data is very important, because it enables us to detect precisely when $MoS_2$ starts to form. The temperature of formation is determined not only by inspecting the spectra, but also by analyzing the Mo–S and Mo–Mo distances. A comparison of the formation of $MoS_2$ in the various catalysts showed that NTA and EDTA have opposite effects on the sulfidation of Mo (Figs. 4 and 5). In catalysts prepared with NTA, $MoS_2$ is formed at lower temperatures, whereas EDTA retards the formation of $MoS_2$. At the concentrations NTA : Ni = 1 and EDTA : Ni = 1, Mo is not complexed by the ligands, because they preferentially bind to Ni. Therefore, the shift in the formation temperature of $MoS_2$ must be due instead to an interaction of Mo with Ni or with the support. The answer to the question concerning the consequences that a shift in the formation temperature of Mo has on the final $MoS_2$ slabs can be found in the Mo *K*-edge EXAFS data. The results of the fits show that the catalyst in which $MoS_2$ is formed at the lowest temperatures (NiMoNTA 1.0) is the one with the highest Mo–S coordination number and the lowest Mo–Mo Debye–Waller factor. The high coordination number indicates a complete saturation of the $MoS_2$ edges, whereas the low Debye–Waller factor points to a high order of the $MoS_2$ slabs. A high regularity of the Mo–Mo distances and a narrow particle size distribution can induce a decrease in the Debye–Waller factor.

A comparison of the XAFS data with the results of the HDN reaction (Table 2) shows a clear correlation between the order of the $MoS_2$ particles and the HDN catalytic performance. The NiMoNTA 1.0 catalyst is the most active for HDN but one of the least active catalysts for the cyclohexene hydrogenation. An explanation of these activity profiles must be sought in the mechanism of the HDN reaction (Fig. 1). The rate-determining step of the HDN of o-toluidine is the hydrogenation of the phenyl ring, which leads to the formation of MCHA. MCHA then reacts quickly to MCHE and MCH. Hydrogenation of olefins (CHE) over sulfided Mo catalysts takes place relatively easily, occurring already at 1 atm pressure of hydrogen. Contrary to olefins, hydrogenation of aromatics requires high pressures of hydrogen. The highest conversion of TOL is obtained with the catalyst which is least active in the hydrogenation of CHE and vice versa. This observation indicates that different sites are involved in the two reactions, as already suggested by Voorhoeve and Stuiver (35). Catalysts active for olefin hydrogenation are not always capable of catalyzing aromatic hydrogenation (36). The dissimilar activity for the two reactions may be due to different degrees of adsorption for the two compounds. The CHE can form an $\sigma$-bond with Mo and Ni, while the aromatic ring is more likely to be $\pi$-bonded to the metal atoms. TOL should adsorb parallel to the edge plane of $MoS_2$, in $\eta^6$-adsorption mode. A more crystalline structure of the active phase might favor the planar adsorption and, thus, the hydrogenation of toluidine. The EXAFS results show that the catalyst with the highest crystallinity is the one containing NTA with a molar ratio of NTA : Ni = 1 followed by the other NTA catalyst. The dried catalyst, prepared in the absence of ligands, showed the most amorphous structure and, at the same time, the lowest HDN activity. The adsorption of the aromatic ring is enhanced by the regularity of the edges of $MoS_2$. On the contrary, the irregular Mo–Mo distances in the catalyst prepared without ligands make the adsorption of the ring more unlikely.

This consideration does not affect the HDS of thiophene because it is assumed that thiophene adsorbs on the catalyst by means of the S atom present in the heterocyclic ring. Therefore, as for the hydrogenation of cyclohexene, the regularity of the catalyst surface does not play a particularly important role.

### *Nickel*

From the Ni *K*-edge QEXAFS measurements, we saw that the sulfidation of Ni in the various catalysts proceeds at different rates. In the catalyst containing NTA, Ni is sulfided at much lower temperatures than in the other catalysts. From the QEXAFS spectra of the fresh catalysts, it is clearly visible that, in the catalysts containing NTA and EDTA, Ni is complexed by the ligands, because the Ni–C shell is detected at around 2.3 Å (phase not corrected). The difference in the sulfidation behavior between the NTA- and the EDTA-containing catalysts can be explained by the higher stability of the EDTA complexes. However, the sulfidation mechanism could be the same for both kinds of catalysts. The presence of chelating ligands probably has an important influence on the sulfidation mechanism of Ni. The change in the sulfidation mechanism also has consequences for the final structure of nickel. Since the chelating ligands tend to isolate Ni from the environment, it is likely that, in the absence of chelating ligands, Ni tends to form larger clusters, whereas the presence of the chelating ligands favors a better dispersion of Ni on the $MoS_2$ crystallites.

A difference in HDS activity is observed between the catalysts containing NTA with the molar ratios NTA : Ni = 1 and NTA : Ni = 1.5 even though they show a similar sulfidation profile for Ni. This suggests that not only is the sulfidation temperature of Ni an important factor for obtaining a higher Ni dispersion, but an increase in the amount of ligand in the catalyst precursor can also have a beneficial effect. However, when there is an excess of ligands, they interact with Mo and have a negative effect on the HDS performance, as shown in previous work (5, 7).

*The Role of Chelating Ligands*

The sequence for the sulfidation of Ni in the various catalysts is the same as for the formation of $MoS_2$, as can be seen in Figs. 5 and 10. In the absence of chelating ligands, Ni can interact either with the support or with molybdenum species. Interactions of Ni with the support would change the properties of the alumina surface so that the adsorption of Mo on $Al_2O_3$ would also be influenced. Another explanation for the observed correlation between the sulfidation temperature of Ni and Mo might be that, in the absence of chelating ligands, Ni-heteropolymolybdates are formed, which are Keggin-type structures consisting of 12 octahedral $MoO_6$ units surrounding a $SiO_4$, $PO_4$, or $AlO_4$ tetrahedron (37).

NTA and EDTA hinder the interaction of $Ni^{2+}$ with the surrounding environment, be it support or molybdenum oxide. This effect was also observed for the silica-supported catalysts (7). A comparison of the data of the catalysts supported on $SiO_2$ and $\gamma$-$Al_2O_3$ allows us to deduce whether Ni interacts with the support or is included in Ni-heteropolymolybdate clusters. On silica, NTA and EDTA had the same effect on Ni: they shifted its sulfidation to higher temperatures in comparison to the catalyst prepared without ligands. On alumina, on the contrary, NTA shifts the sulfidation of Ni toward lower temperature, while EDTA shifts it to higher temperature in comparison to the uncalcined catalyst prepared in the absence of ligands. The temperature of sulfidation of Ni depends on the stability of the compound that Ni forms in the oxidic state. In the absence of ligands Ni is sulfided at a lower temperature on the silica-supported catalyst than on the alumina catalyst. The only difference between the two cases is the support. Therefore, these observations suggest that Ni interacts with the support when no chelating ligands are employed. These observations also indicate that Ni-heteropolymolybdates are not formed. In fact, the presence of Ni-heteropolymolybdates would imply that Ni be sulfided at the same temperature on alumina and on silica when no chelating ligands are used. This confirms the EXAFS and UV-VIS observations of an interaction between Ni and $SiO_2$ (5). In the present work, we could not prove that an interaction between Ni and $Al_2O_3$ exists, but we can deduce it from the mentioned observations. It is noteworthy that on the alumina-supported EDTA- and NTA-containing catalysts, Ni is sulfided at a temperature, which is about 50°C lower than on the corresponding silica-supported catalysts. This may be caused by an interaction between NTA or EDTA with Al cations. This extra driving force for decomposition of the $(NiNTA)^-$ and $(NiEDTA)^{2-}$ complexes lowers the sulfidation temperature of Ni.

The question arises how the chelating ligands can influence the temperature of sulfidation of Mo, since the organic molecules preferentially form complexes with Ni and not with Mo. The answer to this question can be found in the interactions between the various elements composing this catalytic system. In (7) we saw that an increase of the amount of ligands caused a broadening of the sulfidation range of Mo on $SiO_2$. Especially, the onset of the sulfidation was shifted to lower temperature. The sulfidation range of Mo in $NiMo/SiO_2$ catalysts containing the highest amounts of ligands was as broad as that of the $Mo/SiO_2$ catalyst, while the sulfidation range of uncalcined $NiMo/SiO_2$ was considerably narrower. At high ligand concentrations, Ni is completely isolated from the environment because of the chelating effect. When Ni is complexed by ligands, as well as in the absence of Ni, Mo will interact with the support and form compounds that have a larger sulfidation interval. In contrast, in the $NiMo/SiO_2$ catalyst prepared in the absence of ligands, Ni interacts with the support and changes the surface properties of the support. As a result, the Mo–support interactions are influenced. This explanation was confirmed by the use of ethylene diamine as chelating ligand (7), which showed a similar effect as NTA even though it does not form any complex with Mo.

This explanation is based on observations made on $SiO_2$-supported catalysts, for which we could clearly observe the beginning and the end of the sulfidation interval of Mo in the QEXAFS spectra. In the present work on alumina-supported catalysts, we could only precisely detect the formation of $MoS_2$, i.e., the end of the sulfidation interval. The effect of ligand on the sulfidation temperature of $MoS_2$ was found to be the same as for the sulfidation of Ni; NTA aids the formation of $MoS_2$, while EDTA retards it. This suggests that the end of the sulfidation of Mo is closely dependent on the sulfidation of Ni. This would imply that a Ni–Mo interaction is formed during the sulfidation process. It is clear that the sulfidation of Mo is a complex process which is influenced on the one hand by the interactions between the metal ions and the support and, on the other hand, by the sulfidation behavior of Ni.

## CONCLUSIONS

The QEXAFS and EXAFS results enabled us to add to the body of knowledge on the effect of chelating ligands obtained from the study of $SiO_2$-supported NiMo catalysts to $\gamma$-$Al_2O_3$-supported catalysts. Moreover, we compared

the effect of the chelating agents on two hydrotreating reactions, hydrodenitrogenation and hydrodesulfurization.

The HDN catalytic performance is strongly enhanced by the use of NTA. This ligand is believed to cause a decrease in the temperature of formation of $MoS_2$ during the sulfidation process, which enables the development of more regular $MoS_2$ slabs, on which the hydrogenation of o-toluidine is enhanced. The improvement in activity obtained in the HDS of thiophene is limited. Nevertheless, for this reaction, too, a trend was observed in the performance of the catalysts. The improvement in HDS activity was ascribed to the presence of NTA and EDTA. The ligands are believed to bring about a change in the sulfidation mechanism of Ni and a subsequent higher dispersion of the promoter.

The different trend in the HDN and HDS reactions was explained by the fact that, for the HDN reaction, the adsorption and hydrogenation of o-toluidine on $MoS_2$ is the rate determining step, and this step is enhanced by the presence of more regular $MoS_2$ crystallites. In contrast, for the HDS of thiophene, the presence of a greater Ni dispersion plays a more important role.

The collected QEXAFS data, together with the previous data concerning the silica-supported catalysts, allowed us to understand that the main role of the chelating ligands is to hinder interactions between Ni and the environment, which has an indirect influence on the sulfidation of Mo. Ni is believed to interact with the support when no ligands are employed. The similar sulfidation sequence of Mo and Ni in the presence and absence of ligands suggested that the sulfidation of Mo is affected by the sulfidation of Ni.

## ACKNOWLEDGMENTS

The authors thank the staff of the Swiss Norwegian Beam Line at ESRF and the staff of the X1 station at HASYLAB for their technical support and their kind help. This project was supported by the Swiss National Science Foundation.

## REFERENCES

1. Thompson, M. S., European Patent Application 0.181.035 (1986).
2. van Veen, J. A. R., Gerkema, E., van der Kraan, A. M., and Knoester, A., *J. Chem. Soc., Chem. Commun.* 1684 (1987).
3. Medici, L., and Prins, R., *J. Catal.* **163**, 28 (1996).
4. Medici, L., and Prins, R., *J. Catal.* **163**, 38 (1996).
5. Cattaneo, R., Shido, T., and Prins, R., *J. Catal.* **185**, 199 (1999).
6. Cattaneo, R., Shido, T., and Prins, R., *Stud. Surf. Sci. Catal.* **127**, 421 (1999).
7. Cattaneo, R., Weber, Th., Shido, T., and Prins, R., *J. Catal.* **191**, 225 (2000).
8. Kishan, G., Coulier, L., de Beer, V. H. J., van Veen, J. A. R., and Niemantsverdriet, J. W., *J. Chem. Soc., Chem. Commun.* **13**, 1103 (2000).
9. Coulier, L., de Beer, V. H. J., van Veen, J. A. R., and Niemantsverdriet, J. W., *Top. Catal.* **13**, 99 (2000).
10. Clausen, B. S., Topsøe, H., Candia, R., Villadsen, J., Lengeler, B., Als-Nielsen, J., and Christensen, F., *J. Phys. Chem.* **85**, 3868 (1981).
11. Satterfield, C. N., and Yang, S. H., *Ind. Eng. Chem. Process Des. Dev.* **23**, 11 (1984).
12. Perot, G., *Catal. Today* **10**, 447 (1991).
13. Rota, F., and Prins, R., *Stud. Surf. Sci. Catal.* **127**, 319 (1999).
14. Rota, F., and Prins, R., *Top. Catal.* **11/12**, 327 (2000).
15. Rota, F., and Prins, R., *J. Mol. Catal.* **162**, 367 (2000).
16. Prins, R., de Beer, V. H. J., and Somorjai, G. A., *Catal. Rev.-Sci. Eng.* **31**, 1 (1989).
17. Chianelli, R., Daage, M., and Ledoux, M. J., *Adv. Catal.* **40**, 177 (1994).
18. Topsøe, H., Clausen, B. S., and Massoth, F. E., "Hydrotreating Catalysis." Springer Verlag, Berlin, 1996.
19. Startsev, A. N., *Catal. Rev.-Sci. Eng.* **37**, 353 (1995).
20. Schulz, H., Schon, M., and Rahman, N. M., *Stud. Surf. Sci. Catal.* **27**, 201 (1986).
21. Hargreaves, A. E., and Ross, J. R. H., *J. Catal.* **56**, 363 (1979).
22. McCarthy, K. F., and Schrader, G. L., *J. Catal.* **117**, 246 (1987).
23. Startsev, A. N., Burmistrov, V. A., and Yermakov, Y. L., *Appl. Catal.* **45**, 191 (1988).
24. Daly, F. P., *J. Catal.* **51**, 221 (1981).
25. Geneste, P., Amblard, P., Bonnet, M., and Graffin, P., *J. Catal.* **61**, 1015 (1980).
26. Sauer, N. N., Markel, E. J., Schrader, G. L., and Angelici, R. J., *J. Catal.* **117**, 295 (1989).
27. Hensen, E. J. M, Vissenberg, M. J., de Beer, V. H. J., van Veen, J. A. R., and van Santen, R. A., *J. Catal.* **163**, 429 (1996).
28. Tröger, L., *Synchr. Rad. News* **6**, 11 (1997).
29. Kampers, F. W. H., Maas, T. M. J., van Grondelle, J., Brinkgreve, P., and Koningsberger, D. C., *Rev. Sci. Instrum.* **60**, 2645 (1989).
30. Vaarkamp, M., Linders, J. C., and Koningsberger, D. C., *Physica B* **208 & 209**, 159 (1995).
31. Zabinsky, S. I., Rehr, J. J., Ankudinov, A., Albers, R. C., and Eller, M. J., *Phys. Rev. B* **52**, 2995 (1995).
32. Ankudinov, A. L., and Rehr, J. J., *J. Phys. Rev. B* **56**, 1712 (1997).
33. Wignacourt, J. P., Drache, M., Swinnea, J. S., Steinfink, H., Lorriaux-Rubbens, A., and Wallart, F., *Can. J. Appl. Spectrosc.* **37**(2), 49 (1992).
34. Mueller, A., Pohl, S., Dartmann, M., Cohen, J. P., Bennett, M. J., and Kirchner, R. M., *Z. Naturforsch.* **34**, 434 (1979).
35. Voorhoeve, R. J. H., and Stuiver, J. C. M., *J. Catal.* **23**, 228 (1971).
36. Krishnamurthy, S., Panvelker, S., and Shah, Y. T., *AIChE J.* **27**, 994 (1981).
37. Greenwood, N. N., and Earnshaw, A., "Chemistry of the Elements." Pergamon Press, New York, 1986.